

General Disclaimer

One or more of the Following Statements may affect this Document

- This document has been reproduced from the best copy furnished by the organizational source. It is being released in the interest of making available as much information as possible.
- This document may contain data, which exceeds the sheet parameters. It was furnished in this condition by the organizational source and is the best copy available.
- This document may contain tone-on-tone or color graphs, charts and/or pictures, which have been reproduced in black and white.
- This document is paginated as submitted by the original source.
- Portions of this document are not fully legible due to the historical nature of some of the material. However, it is the best reproduction available from the original submission.

NASA CR-144818

FINAL REPORT
TO
NATIONAL AERONAUTICS AND SPACE ADMINISTRATION
FOR
CONTRACT NAS 5-20492

SUPPORT OF THE INFRARED RADIOMETER ON THE ST

G. Neugebauer
M. W. Werner
Principal Investigators

July 15, 1976

California Institute of Technology
Department of Physics
Pasadena, California 91125

(NASA-CR-144818) SUPPORT OF THE INFRARED
RADIOMETER ON THE ST Final Report, 10 May
1974 - 30 Nov. 1975 (California Inst. of
Tech.) 36 p HC A03/MF A01 CSCL 14B

N77-12361

G3/35
Unclas
54622
RECEIVED
NASA STI FACILITY
INPUT BRANCH

6 910117273

1. Report No.	2. Government Accession No.	3. Recipient's Catalog No.	
4. Title and Subtitle		5. Report Date	6. Performing Organization Code
SUPPORT OF THE INFRARED RADIOMETER ON THE ST		July 15, 1976	
7. Author(s)	8. Performing Organization Report No.		
G. Neugebauer and M. W. Werner			
9. Performing Organization Name and Address		10. Work Unit No.	
California Institute of Technology Department of Physics Pasadena, California 91125		11. Contract or Grant No.	
		NAS 5-20492	
12. Sponsoring Agency Name and Address		13. Type of Report and Period Covered	
Goddard Space Flight Center Greenbelt, Maryland 20771		Final 5-10-74/11-30-75	
15. Supplementary Notes		14. Sponsoring Agency Code	
Dr. Tom Kelsall			
16. Abstract			
<p>This report covers a one-year study of particular elements of interest in connection with the infrared radiometer proposed for the ST. The aim of the contract was to obtain practical experience, including observational experience, with bolometers suitable for the long wave infrared and with the filters necessary to define the spectral regions of interest. The techniques used in fabricating and testing bolometers and filters are described, and the results which have been obtained to date are discussed.</p>			
17. Key Words (Selected by Author(s))		18. Distribution Statement	
Far infrared detectors - far infrared filters.			
19. Security Classif. (of this report)	20. Security Classif. (of this page)	21. No. of Pages	22. Price*
		36	

Figure 2. Technical Report Standard Title Page

PREFACE

This report covers a one-year study of particular elements of interest in connection with the infrared radiometer proposed for the ST. The aim of the contract was to obtain practical experience, including observational experience, with bolometers suitable for the long wave infrared and with the filters necessary to define the spectral regions of interest. Since the two phases were distinct, the reports on each is contained in a separate chapter.

The objective of the bolometer development was to try to approach the theoretical sensitivity limits of bolometer working at the long infrared wavelengths ($30\mu < \lambda < 1 \text{ mm}$). The scope included fabrication, testing and field use of appropriate detectors. While the techniques we used made detectors which were significant improvements over previous bolometers and produced bolometers which were usable in millimeter astronomical research, they did not achieve the theoretical sensitivity. The general concept of composite bolometers has been verified but further study of the noise properties, the absorption efficiency, and fabrication techniques is necessary. A portion of this chapter was written by M. Hauser who participated in the bolometer development at Caltech prior to the beginning of this contract.

The objectives of the filter study were to explore techniques for reliably making and testing filters of moderate bandwidth for use at the long infrared wavelengths. The scope of the work was limited to mesh Fabry-Perot filters for use between 200μ and 1 mm . A straightforward fabrication technique was evolved which can produce filters approaching those desired for the ST. Figure work on very flat spacers, capacitive mesh filters, and long wavelength blocking filters is suggested. This portion of the work was largely done by J. Elias, a graduate student at Caltech.

TABLE OF CONTENTS

List of Illustrations	1
List of Tables	1A
Chapter 1 - Composite Bolometers	
Introduction	2
Bolometer Construction	6
Test Procedures and Results	11
Summary	17
Chapter 2 - Filters	
Introduction	21
Program of Work	23
Commercially Available Filters	34
Summary	34
Bibliography	37

LIST OF ILLUSTRATIONS

	Page
1. Schematic Drawing of Bolometer	4
2. Calculated Optical Parameters for Thin Films	7
3. Assembly of Composite Bolometer	9
4. Circuit for Measuring and Typical Examples of Bolometer Load Curves	13
5. Low Noise FET Preamp	14
6. Schematic of Test Setup for Bolometers	16
7. Overall Wavelength Response of System Shown in Figure 6	26
8. Schematic of Typical Filter	28
9. Transmission Curve for Narrow Band Filter	31
10. Transmission Curve for High Pass Filter	32
11. Transmission Curve for Narrow Band Filters	33

LIST OF TABLES

	Page
Table 1. Bolometer Characteristics	18, 19
Table 2. Filter Parameters	36

Chapter 1

COMPOSITE BOLOMETERS

I. Introduction and Motivation

The infrared radiometer proposed for the ST is intended to work at wavelengths from $1\text{ }\mu$ to 1 mm . Detection of this radiation is optimally achieved using two or more detectors. At wavelengths $\leq 30\text{ }\mu$ photoconductors are available which have intrinsic sensitivities at most wavelengths where they are sensitive, much better than the limit set by fluctuations in the radiation of the warm mirror. For wavelengths longer than $\sim 30\text{ }\mu$ photoconductors are no longer sensitive and bolometers must be used.

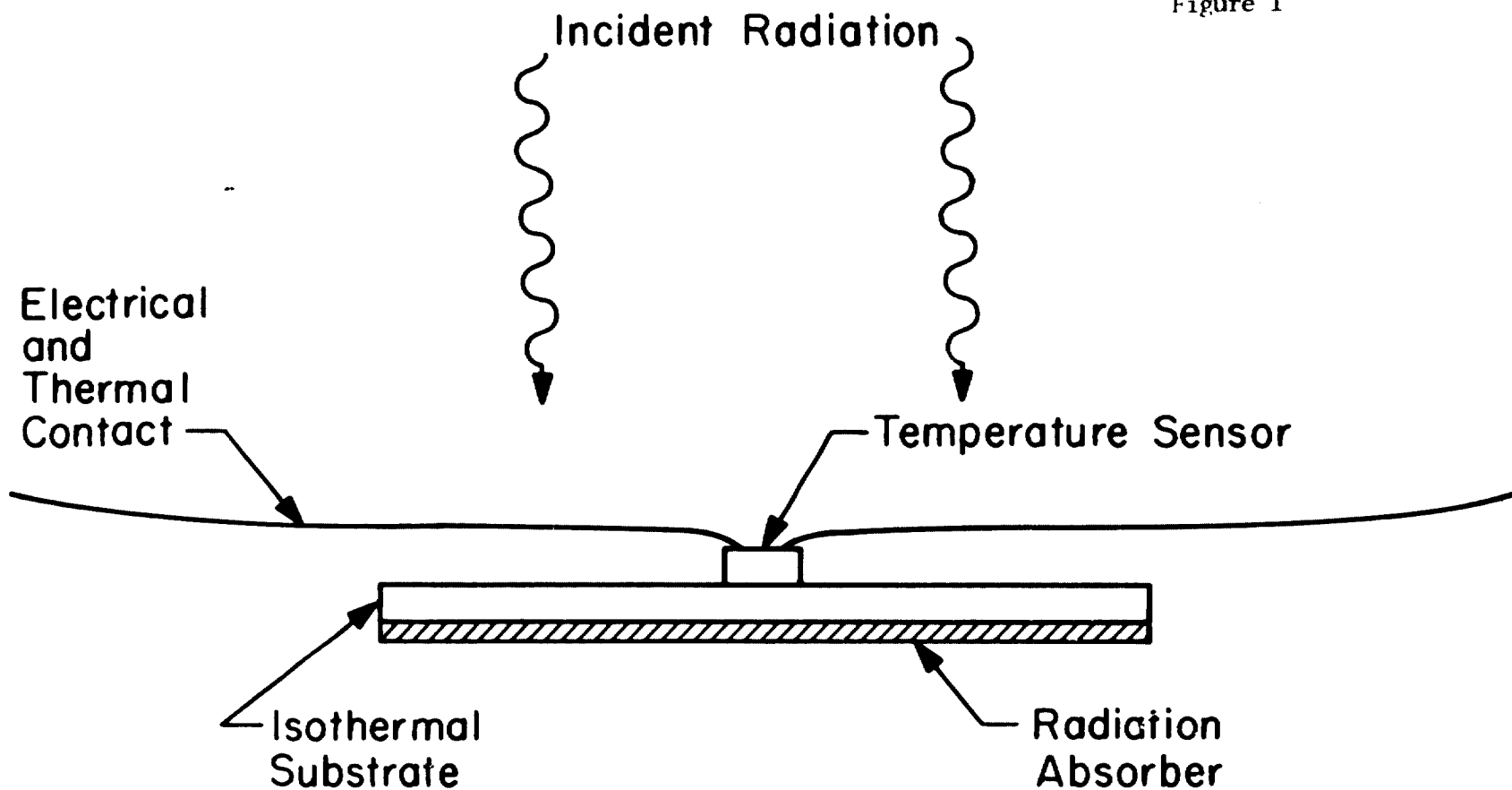
Although the conventional doped-germanium bolometer used by astronomers for many years (Low 1961) for wavelengths $\lambda \leq 100\text{ }\mu$ will operate at long wavelengths, one pays a penalty in sensitivity as the long wavelength limit is increased. This penalty occurs because the volume of the bolometer (and hence its heat capacity) must be increased as the wavelength increases: the thickness to maintain high radiation opacity, and the area of, encompass the increasing image size. For constant telescope size and illumination solid angle of the detector, the detector area required to intercept the diffraction-limited image grows as λ^2 . The sensitivity (detectivity) of a bolometer designed to operate at a specified temperature with a specified thermal time constant will vary inversely as the square root of the detector volume, assuming the heat capacity is dominated by the semiconductor element itself.

It has been recognized for some time that bolometer performance at long wavelengths could be improved if efficient

radiation absorption could be achieved with a substrate whose properties are independent of those of the temperature-sensitive element (Low 1970; Coron, Dambier, and LeBlanc 1972). The success of this approach in practice depends upon the ability to construct an absorber of the required area having lower heat capacity than the corresponding volume of germanium or silicon, and upon the ability to establish good thermal contact between such an absorber and the temperature-sensitive element without introducing significant excess noise. We refer to bolometers in which the radiation absorption and temperature-sensing regions are distinct as composite bolometers.

Prior to the period of this contract, a type of composite bolometer incorporating the familiar germanium bolometer had been developed in our laboratories for use in a ground-based observing program at 1 mm (Hauser and Notarys 1975). The initial results were quite encouraging, yielding a bolometer with far infrared radiative NEP of 6×10^{-14} watts $\sqrt{\text{Hz}}$, a factor of 2-3 better than our conventional germanium bolometer of comparable size.

The composite bolometer developed in our laboratory is shown schematically in Figure 1. The bolometer consists of a small germanium crystal attached to a sapphire substrate with a resistive film coating (substrates of this type were described by Clarke, Hoffer and Richards 1974). The resistive film has a surface impedance chosen to provide efficient radiation absorption, and the sapphire provides a mechanical support having a low thermal mass and high thermal diffusivity. The two lead wires attached to the germanium crystal support the entire detector, provide electrical contact for bias and signals, and provide the thermal contact between the bolometer and its temperature reservoir.



COMPOSITE BOLOMETER

Figure 1: Schematic Drawing
of Bolometer

Bolometers of this type built both before the period of this contract and under the support of the contract have been successfully used for observations at millimeter and submillimeter wavelengths on the 5 m telescope at Mt. Palomar and on the 1.5 m Caltech sky survey telescope, which has been used both at Mauna Kea and, more recently, at White Mountain. The bolometers have proven to be durable and have survived both many thermal cycles and many trips to remote sites. The results obtained with these bolometers at the telescope are a factor of 1.5 to 2 better than have been obtained with any comparable detection system which has been used for ground-based observations. Specifically, on the 5 m telescope, with the detectors described below, and 2 to 3 pr mm of atmospheric H₂O in the line of sight, we are able to reach a limiting flux of 0.5 Jy in one hour of integration. These results have formed the basis of several scientific publications (e.g. Werner et al. 1975; Westbrook et al. 1976).

In the following, we describe the fabrication techniques and the results obtained. We have not been able to produce and test the large number of bolometers required for a systematic exploration of the effects of varying all parameters. Therefore, we have described in detail the test procedures used and the properties of the best bolometers, in order to show what can be achieved; we also indicate some of the outstanding problems we have encountered.

II. Bolometer Construction

The sapphire substrates for the bolometers we have built are highly polished squares approximately 2 mm on a side, with thickness of 0.1 mm. The heat capacity of this substrate at 1.8 K is approximately $0.9 \times 10^{-9} \text{ JK}^{-1}$ compared with $7 \times 10^{-9} \text{ JK}^{-1}$ for a piece of germanium of the same size. In this thickness germanium would have a low absorption efficiency at 1 mm.

The resistive films are made of bismuth, which is easy to apply in the required thicknesses (of order 10^3 \AA) though soft and therefore fragile. The required surface resistance of the film depends upon the index of refraction of the substrate and the character of the desired spectral response. Figure 2 shows calculated power absorption, reflection, and transmission coefficients for normal incidence as a function of optical thickness, $\frac{2\pi}{\lambda} nt$, for a substrate with index of refraction $n = 3$ and thickness t . The parameter labeling each curve is the ratio of surface resistance of the film, R (in ohms per square), to the free space wave impedance R_0 (377 ohms). These curves can be extended to larger thicknesses by noting that they are periodic functions symmetric about $\pi/2$. The calculations assume operation in the "low frequency" radiation limit, i.e. in the limit in which the magnitude of the wave impedance in the resistive medium is much less than R_0 and in which the film thickness is small compared to the skin depth. These curves show that in general one obtains "fringes" in the spectral absorption coefficient. However, for the special case $R/R_0 = (n-1)^{-1}$ (the curve labeled 1/2 in Figure 2), the fringe amplitude is zero and one has a flat spectral response with 50 percent absorption. For sapphire the index of refraction in the far

Radiation Absorption in Thin Resistive Films

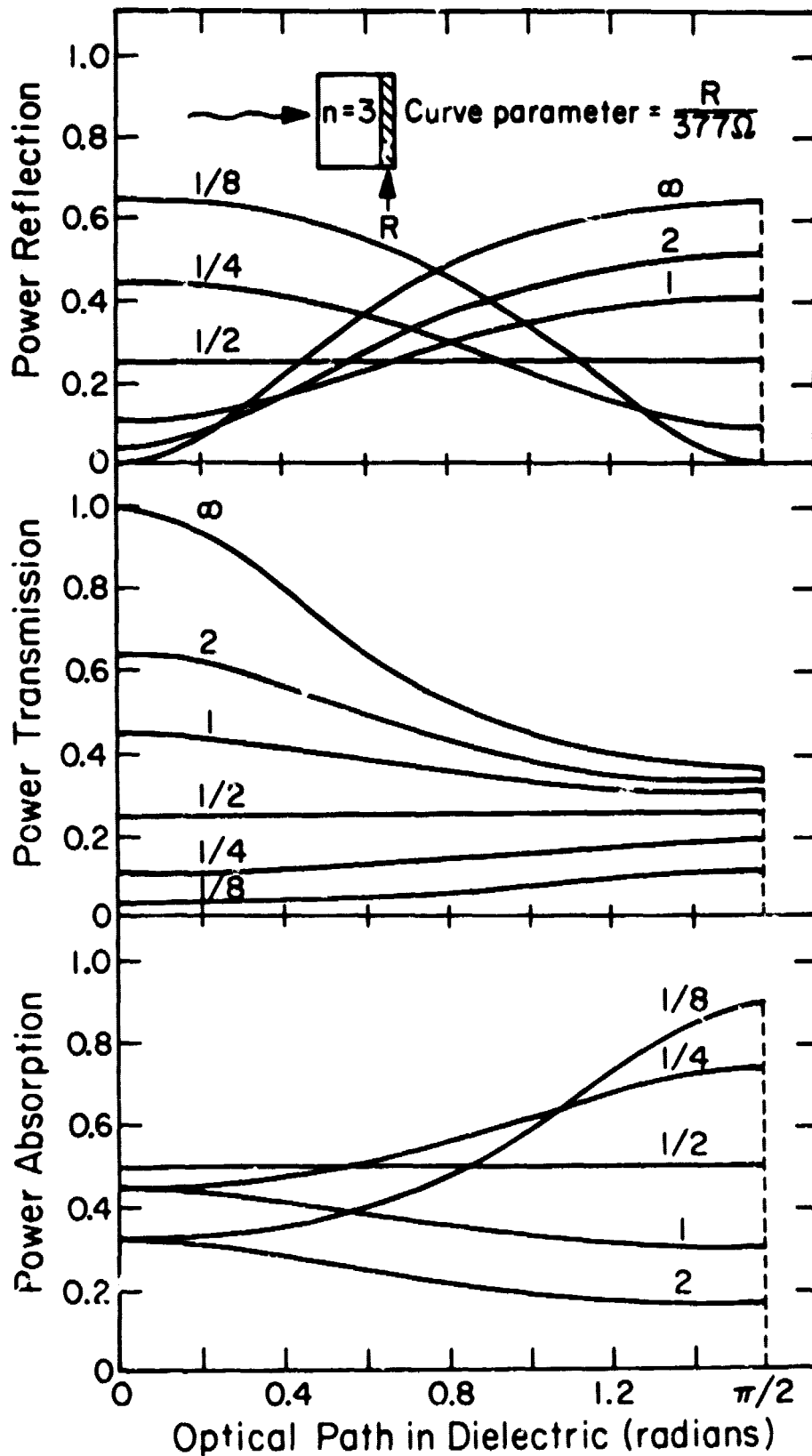


Figure 2: Calculated Optical Parameters for Thin Films

infrared is approximately 3.2, implying flat response for $R = 172$ ohms per square, the design value chosen for our bolometers. This value is achieved by performing test evaporations on sapphire beginning with different known quantities of bismuth, and then measuring the sheet resistance of the film (at 4 K). The optical performance was verified by making transmission measurements and comparing with the curves of Figure 2.

The temperature sensor is a standard germanium bolometer, approximately 0.4 mm x 0.4 mm x 0.1 mm in size. Most of the germanium chips used in our detectors were cut from a boule doped with gallium ($1.5 \times 10^{16} \text{ cm}^{-3}$) and compensated with antimony ($1.5 \times 10^{15} \text{ cm}^{-3}$). For operation at 1.8 K these chips typically have a temperature coefficient of resistance, $\frac{d \ln R}{dT}$, of 2.5 K^{-1} , and a dc resistance at 1.8 K of 2 to 10 M Ω with no bias power applied. Both brass and tungsten lead wires have been used, typically 10 μm to 30 μm diameter depending upon the thermal conductance required. For example, 0.5 μm tungsten leads 1 cm in length give thermal conductance of 0.3 $\mu\text{W K}^{-1}$ near 1.8 K. The leads are attached with a 50-50 In-Sn solder after cleaning the chips with CP 4 etchant. All of the fabrication operations are done by hand under a low power microscope, requiring considerable skill and patience on the part of the technician.

The work under this contract has led to improved techniques for bolometer fabrication which have a high rate of success. The assembly is carried out as indicated in Figure 3. The first step is to lay a quartz fiber between two pads which are placed on the copper block which will hold the assembled bolometer. One of the pads is conducting epoxy,¹ and the

¹Eccobond 56C, available from Emersor and Cuming, Inc. Cantron, Massachusetts.

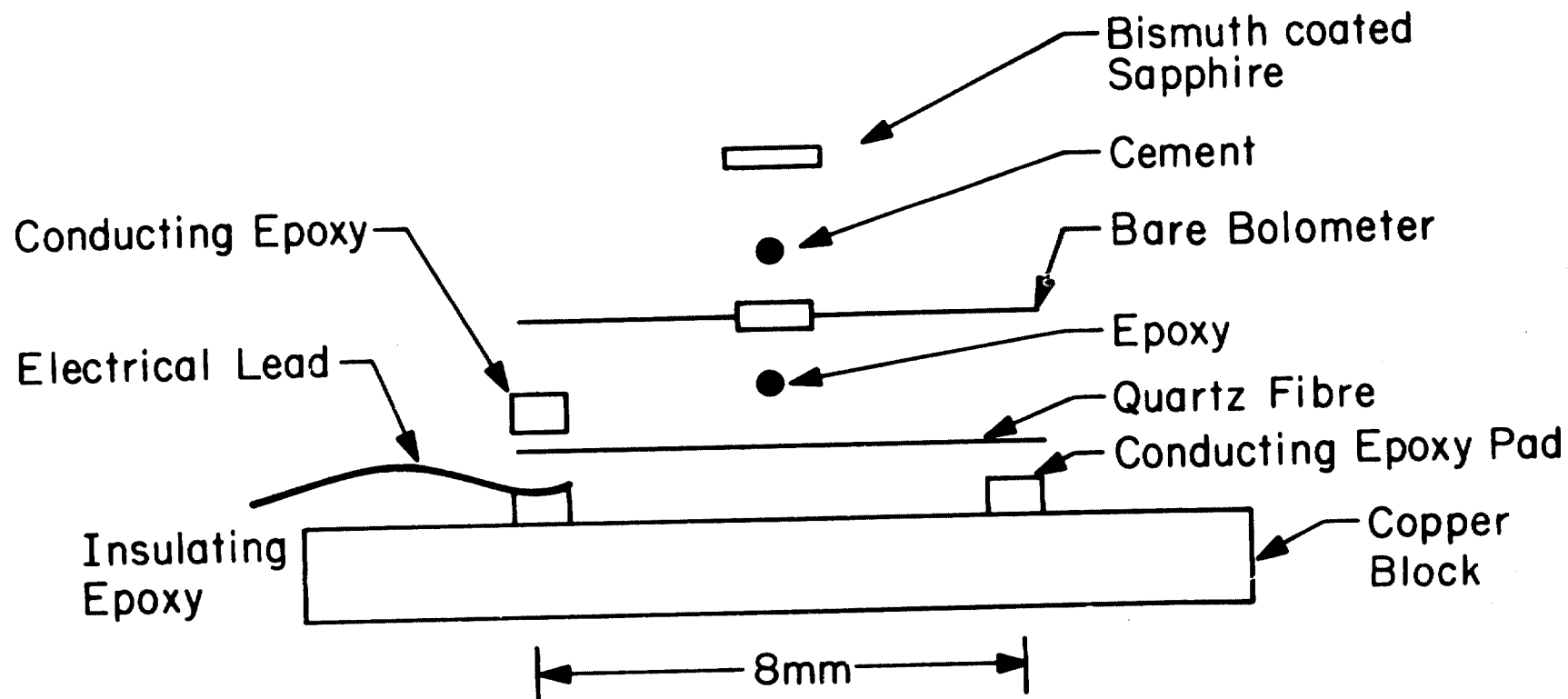


Figure 3: Assembly of Composite
Bolometer

other pad is non-conducting epoxy.² The bare bolometer, with leads attached but without the sapphire substrate, is laid upon the quartz fiber; a small dab of non-conducting epoxy between the fiber and the bolometer provides mechanical support for the structure. One of the bolometer leads is pressed into the conducting epoxy pad to make a ground connection, while the other is pressed into a conducting epoxy pad atop the insulating epoxy to form a terminal into which the bias current is injected and across which the signal is measured. Finally, the sapphire substrate is glued to the bolometer. Several substances have been used for this glue, as will be described below. Both this glue and the epoxy used to fasten the bolometer to the quartz fiber are used in exceedingly small quantities to minimize their contribution to the heat capacity of the structure. The advantage of this technique is that the bare bolometer is much easier to handle than is the bolometer plus sapphire substrate, and a success rate of 90% in mechanical assembly has been achieved.

If a bolometer of the type and size described above is designed for operation at 1.8 K at a chopping speed of 20 Hz, the thermal conduction noise (noise due to fluctuations in the phonon exchange with the temperature reservoir) and Johnson noise in the resistive element combine to set a lower limit to the achievable NEP of $\sim 10^{-14} \text{ WHz}^{-1/2}$. At a fixed temperature T this limit is proportional to the square root of the chopping frequency, and at a fixed operating frequency it is proportional to $T^{5/2}$. In practice, the bolometers of this type built prior to work under this contract such as bolometer #1 described in detail below, had the expected low heat capacity and high responsivity, but were noisier than the fundamental limits by a factor of ~ 3 or more when completely assembled. The noise of the germanium chip alone

²Epoxipatch, The Dexter Corporation, Olean, New York

(before attachment of the sapphire) was significantly lower. The nature of this excess noise is not understood, but it may have been related to the epoxy which was initially used to cement the sapphire substrate to the bolometer. More recently, lower noise performance has been obtained from bolometers in which either thermal joint compound³ or vacuum grease⁴ was used to fasten the substrate to the bolometer.

The bolometers built under the contract, such as bolometer #2 described below, have had both lower noise and lower responsivity, thus leading to a comparable electrical NEP. Tests of the radiation response in the far infrared are, in the best cases, consistent with the expected 50% absorption efficiency. Additionally, the spectral response appears uniform for a $170 \Omega/\square$ film, as expected from the theory. Thus, the radiative NEPs achieved have been of the order of $\sim 6 \times 10^{-14}$ watts/ $\sqrt{\text{Hz}}$. This is still substantially above the theoretical limiting NEP.

III. Test Procedures and Results

In this section, we describe the test procedure used with the composite bolometers and the results obtained on the best bolometers we have built. This is done in order to permit others to duplicate these measurements. Several measurements are routinely made to test new bolometers; the most important of these are determinations of the d.c. (load curve) voltage-current characteristic, of the electrical noise, and the radiation responsivity as a function of frequency. The load curve is measured by injecting a known variable current into the bolometer and measuring the voltage

³Thermacote, available from Thermalloy Co., Dallas, Texas

⁴Apiezon N Grease, available from J. G. Biddle Co., Plymouth Meeting, Pennsylvania

developed across it. A circuit to accomplish this is shown in Figure 4a. Since these bolometers have high resistance, the voltage measurements must be made with a high ($> 100 \text{ M}\Omega$) input impedance voltmeter. Load curves for two of the better bolometers we have built are shown in Figure 4b, and the results of these and other tests on these bolometers are given in Table I. The load curve is useful because, as shown in Figure 4b, it permits determination of the d.c. responsivity, S_0 (volts/watt), which is the change in voltage across the detector per watt of absorbed power. This can be computed from the tangent to the load curve (Figure 4b) from the formula $S_0 = V_2/211V_1$. Typical values of S_0 are $\sim 5 \times 10^5 \text{ V/W}$ to $2 \times 10^6 \text{ V/W}$.

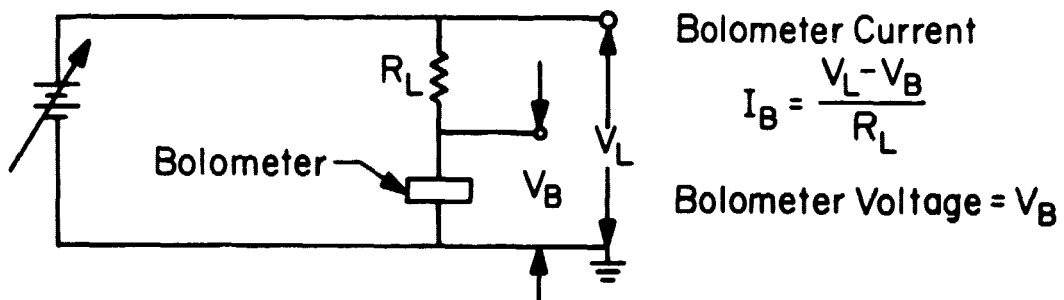
The noise is measured with a frequency tunable voltmeter⁵ which permits the determination of rms noise voltage in a selected bandwidth as a function of frequency. It has proven most convenient to choose a measuring bandwidth of 1 Hz and to measure the noise in this bandwidth at several frequencies, typically 10 and 20 Hz. The bolometers are used with a low noise FET preamp, developed under this contract, which has a gain of 1000 (Figure 5). The preamp allows both the noise and the signal to be measured as a function of bias current. A He temperature load resistor of 5 to 20 $\text{M}\Omega$ is used.⁶ The measured detector noise values are typically in the range of 20 $\text{nV}/\sqrt{\text{Hz}}$ to 70 $\text{nV}/\sqrt{\text{Hz}}$, referred to the preamplifier input. The preamp noise, typically 5 to 7 $\text{nV}/\sqrt{\text{Hz}}$, is negligible on this scale.

The real measure of the quality of a detector is the measured signal-to-noise ratio with standard filtering, field

⁵Infrared Industries Model 601 Tunable Microvoltmeter

⁶Victoreen Mox 400 Resistors, Victoreen Inst., Cleveland, Ohio

a) Measuring Circuit



b) Typical Load Curves

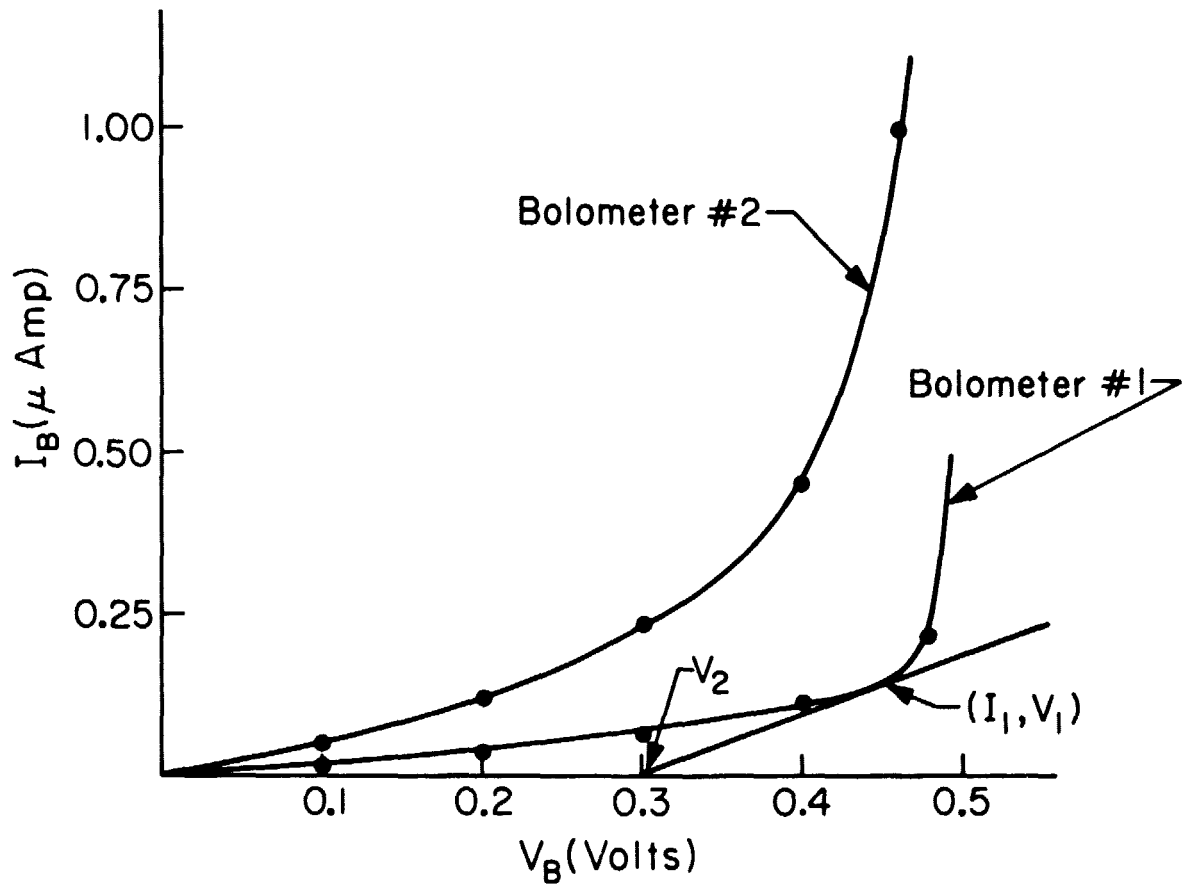
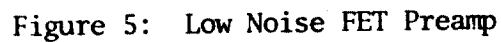


Figure 4: Circuit for Measuring, and Typical Examples of Bolometer Load Curves



optics and a standard radiation source. The dewar configuration and radiation tests we have developed are the following (Figure 6).

A. Field Optics

The detector is tested in a standard vapor cooled or N₂ shielded liquid He dewar.⁷ A standard 12 mm diameter KBr field lens⁸ having a nominal focal length of 8 mm at 10 μ is used; when corrections for the change in refractive index are applied, the focal length at submillimeter wavelengths is ~ 5 mm. This lens is placed behind a 6 mm aperture (Figure 6). The lens and aperture are at He temperature. A 1.25 mm aperture is placed over the bolometer in the focal plane of the field lens.

B. Filtering

A 2.5 mm thick fluorogold⁹ filter is just above the lens, also at He temperature. This defines the basic wavelength response of the system, which responds only to wavelengths beyond 200 μ . The only other optical elements are an 0.1 mm thick black polyethylene filter at the nitrogen temperature shield, and the dewar window itself, which is 1.5 mm thick teflon. The overall wavelength response of this system is shown in Figure 7.

⁷Infrared Laboratories, Tucson, Arizona

⁸Obtainable from John H. Ransom Laboratories, Los Angeles, California.

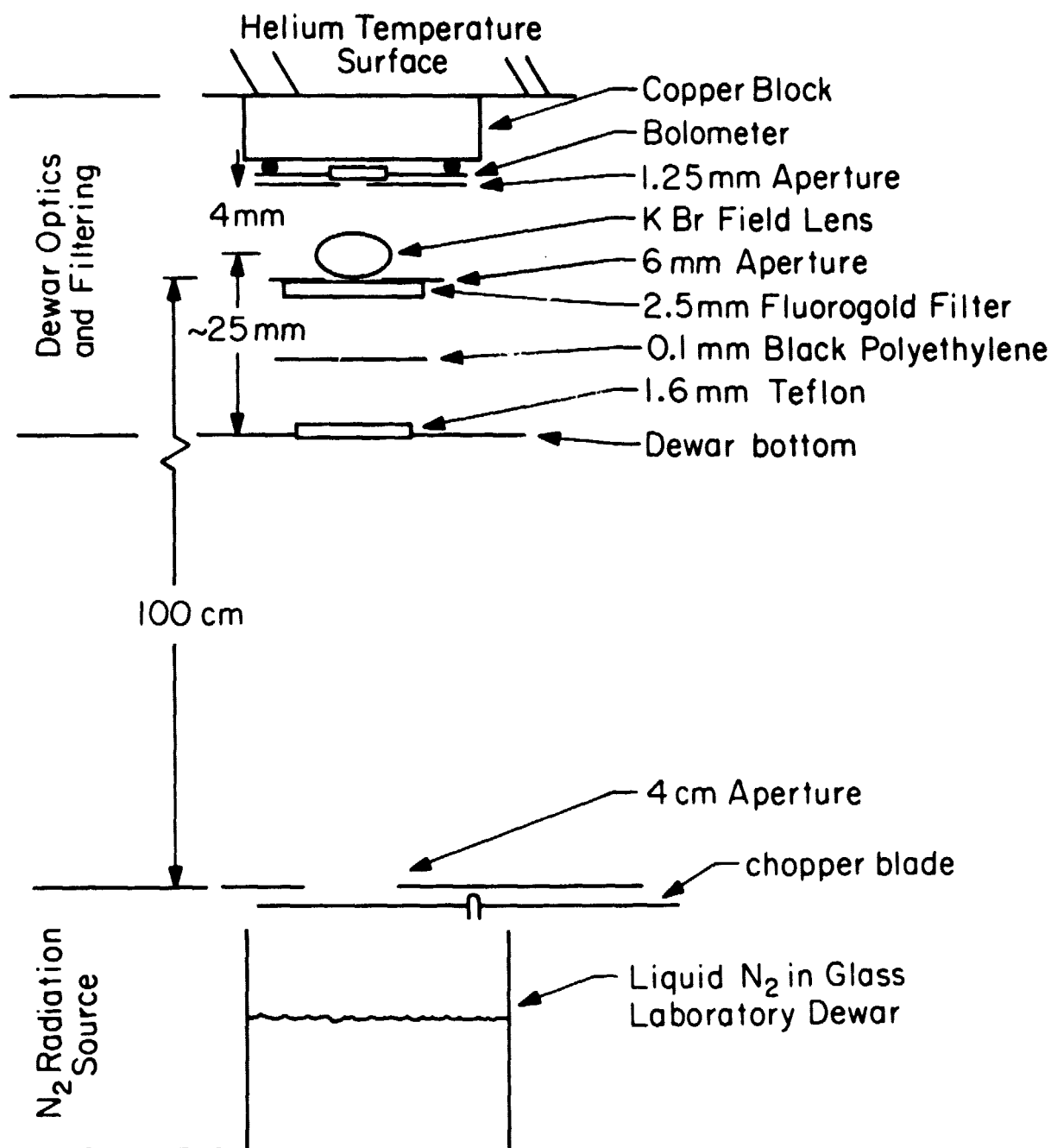


Figure 6: Schematic of Test Set-up for Bolometers

C. Radiation Source

We have found that a glass dewar filled with liquid N_2 is an easy to use and highly reproducible radiation source for these long wavelengths. The detector views the nitrogen through a 4 mm aperture in a blackened plate placed over the dewar (Figure 6). A blackened chopper blade immediately behind this plate permits the radiation from the N_2 source to be modulated (square wave chopping) at frequencies from 5 to 30 Hz. Thus the signal measured by the detector is due to the temperature difference between the liquid N_2 ($T \sim 77$ K) and the chopper ($T \sim 300$ K). The detector is mounted in a down-looking configuration in the dewar, so that it looks out of the bottom of the dewar and views the liquid N_2 source. The distance from the source aperture to the 6 mm aperture over the field lens is 1 m. At this distance, the 4 mm aperture of the N_2 source is effectively a point source, so both the radiation response and the beam pattern of the field optics can be measured in this test configuration. For the detectors (Table I), this leads to a measured signal-to-noise ratio of 1700 for our standard test set up. We also tabulate in Table I the ratio $K = \frac{\text{measured signal}}{\text{dc responsivity}}$, which is a measure of the efficiency of the detector-optics system. Note K is comparable for these two bolometers, but values of K as much as a factor of 2 lower have been noted among the bolometers made here. Since the bolometers have been tested under identical and reproducible conditions, there is a suggestion that the properties of the absorbing bismuth film may not be reproducible.

IV. Summary

We have developed and described techniques for making composite bolometers which are rugged, reliable, and very

TABLE 1 - Bolometer Characteristics

Bolometer Parameters		
	Bolometer #1	Bolometer #2
Sapphire Substrate Size	2mm x 2mm x 0.12mm	2mm x 2mm x 0.12mm
Bismuth Film Resistivity (4° K)	~ 170 Ω/\square	~ 170 Ω/\square
Ge Chip Size	.4mm x .4mm x .12mm	.5mm x .5mm x .08mm
Glue Used to Fasten Ge to Sapphire	Epoxy	Thermal Joint Compound
Leads	.12mm Tungsten, 3mm Length	.3mm Brass, 4mm Length
He Bath Temperature During Test	1.7K	1.9K
Value of He Temperature Load Resistor Used in Test	20 M Ω	5 M Ω

TABLE 1 (cont)

	Bolometer #1	Bolometer #2
Resistance at Bath: Temperature, Zero Bias Current	6 M Ω	1.25 Ω
Optimum Bias Current	.15 μ Amp	.49 μ Amp
DC Responsivity at Opt. Bias	2 x 10 ⁶ V/W	5 x 10 ⁵ V/W
Detector Noise 10 Hz	60 nV/ $\sqrt{\text{Hz}}$	20 nV/ $\sqrt{\text{Hz}}$
20 Hz	50 nV/ $\sqrt{\text{Hz}}$	12 nV/ $\sqrt{\text{Hz}}$
Electrical NEP	3 x 10 ⁻¹⁴ watts/ $\sqrt{\text{Hz}}$	4 x 10 ⁻¹⁴ watts/ $\sqrt{\text{Hz}}$
Radiation Signal, Standard N ₂ Source, 10 Hz	104 μ V	34 μ V
20 Hz	90 μ V	22 μ V
Time Const	7 m sec	9 m sec
Signal/Noise at 10 Hz	1700	1700
$K = \frac{\text{measured radiation signal}}{\text{DC responsivity}}$	52	68

ORIGINAL PAGE IS
OF POOR QUALITY

Bolometer
Test Results.
All voltages
referred to
preamp input.
Test Procedures
described in
text.

useful for ground-based submillimeter and millimeter wavelength observations. Even the best bolometers however, are a factor two to three less sensitive than the theoretical limiting sensitivity. The following areas need to be explored to improve the performance of these bolometers:

- a) the noise is too large, typically by at least a factor of two;
- b) the absorption efficiency of the bismuth films may vary by a factor of two from one bolometer to the next;
- c) the bolometer heat capacity could probably be reduced further by improved fabrication techniques. This would permit lowered thermal conductance and higher sensitivity for the same thermal time constant.

Chapter 2

FILTERS

I. Introduction and Motivation

The present design for the ST infrared photometer includes a series of moderate bandwidth ($\Delta\lambda/\lambda = 0.1$) filter which would cover the region from $1\ \mu$ to about $1\ \text{mm}$. Conventional multilayer dielectric interference filters are available for wavelengths shorter than roughly $35\ \mu$, but for longer wavelengths filter technology is still largely experimental.

Far infrared filter technology is a fairly broad subject, and with the limited manpower and funding we could not hope to cover the field completely. We therefore restricted our work to an area where we felt that some improvement might be made on existing knowledge and techniques. Before proceeding to a description of our work, it would seem useful to provide a brief summary of available techniques and references.

A fairly comprehensive summary of work up through 1971 is given in Moller and Rothschild (1971). Except where given here specifically, references to original work may be obtained from this book.

Most narrow-band filters consist of two components: a narrow-band filter which provides the basic bandpass but also may have short or long wavelength leaks, and a blocking filter which isolates a relatively broad-band. Blocking filters are mostly of two types: either scattering filters, which use particles whose size is comparable to the cut-on wavelength

wavelength (see Armstrong and Low 1974, for discussion and further references); or, filters which make use of the lattice vibration (restrahlen) bands of crystals, either by use of the pure crystal or by mixing powdered material in a polyethylene sheet ("Yoshinaga filter"). If crystals are used, the filter may be used in reflection to isolate a broad-band. These filters are discussed in Moller and Rothschild, and some additional information is given in Armstrong and Low (1973).

The narrow-band filter component is most generally composed of one or more metal mesh elements. These can be either wire grids ("positive" or "inductive" meshes) or their complement, a pattern of squares deposited on a thin substrate ("negative" or "capacitive" meshes). Moller and Rothschild review the properties of these meshes briefly. The most common type of filter uses these meshes as elements in a Fabry-Perot interference filter. The meshes are spaced approximately half a wavelength apart. Early work along these lines is discussed by Moller and Rothschild. Some more recent work of particular interest is described by Holah and Smith (1972) and by Wijnbergen (1973). Filters of this general type can be constructed for wavelengths shorter than 100 μ though the mechanical tolerances become increasingly difficult to meet as the wavelength of peak transmission decreases.

A second type of mesh filter uses the properties of individual inductive meshes, which have a peak in transmission at a wavelength roughly equal to the "wire" spacing in the grid. The bandpass may be improved in shape by using two or more meshes in sequence. The advantage of this type of filter over the Fabry-Perot type is that the spacing between meshes is no longer critical. However, there is much less control over the width of the band. Filters of this type may

well be useful at wavelengths between about 35 μ and 50 μ , but at longer wavelengths the Fabry-Perot filters are preferable.

We felt that the area we could most usefully investigate was the mesh Fabry-Perot, in that such filters are not readily available and techniques of construction are currently either slow or imprecise. We concentrated primarily on filters for use at the longest wavelengths (200 μ to 1000 μ) because mechanical tolerances for this wavelength region are least precise, and because we could also test the filters' durability when used for astronomical observations. What follows is a summary of the work we have done to date.

II. Program of Work

Our filter program consisted of four parts:

- (1) Development of a reliable and accurate test set-up for measuring filter transmission in the far-infrared (20-1000 μ);
- (2) Design and construction of test filters for the long wavelength end of this region (200- 1000 μ) in order to determine whether construction methods were reliable;
- (3) Tests of available commercial filters for the same wavelength region, in order to compare their properties with those of filters produced in (2);
- (4) Depending on the relative success of (2) and (3), development of improved construction techniques, so that filters could be produced faster and more reliably than were the test filters.

Work on the four parts of the program has been carried to various stages of completion.

A. Test Set-Up

Our test set-up consists of a modified commercial Fourier transform spectrometer.¹⁰ The modifications were made primarily to permit maintenance using locally available parts, and were largely substitutions rather than design changes. The only real changes in design were the substitution of a quartz-iodine lamp for the original mercury arc lamp source, and mechanical modifications to permit substitution of an external detector for the Golay cell supplied with the instrument.

Currently, the instrument can be used in two modes. In the first of these, we use the original detector, a Golay cell¹¹ which has an NEP of about $2 \times 10^{-10} \text{ w/Hz}^{1/2}$ or better. The cell response is uniform as a function of wavelength, but the response of the system is reduced at short wavelengths by the use of black polyethylene as a short wavelength rejection filter. In the second mode of operation, an external detector is substituted for the Golay cell. This external detector is usually a bolometer and filter combination whose relative wavelength response we wish to determine by comparing its spectrum with that seen by the Golay cell. The set-up is not suited for determining absolute response.

Although filters were occasionally tested in combination with an external detector, we have no detector system especially constructed for use with the spectrometer.

¹⁰Beckman RLIC FS-720

¹¹Pye Unicam SP 50

An example of a detector comparison is given in Figure 7. This gives the response of bolometer #1, discussed above, in the optical system shown in Figure 6. The detector system contains a liquid helium cooled 2 mm x 2 mm composite bolometer. Short wavelength radiation is eliminated by means of a combination of liquid helium temperature Fluorogold⁹ and liquid nitrogen temperature black polyethylene. The bolometer is located at the focus of a field lens. A 6 mm aperture at the field lens defines the collecting area of the system and also provides a limited amount of long wavelength rejection. The radiative NEP of the bolometer is of the order of $6 \times 10^{-14} \text{ W}/\sqrt{\text{Hz}}$.

The wavelength response of the system is determined by taking spectra with it and with the Golay cell under identical conditions. If the Golay cell has a flat response, the ratio of the two spectra represents the wavelength response of the bolometer and its filtering. This ratio is shown plotted on an arbitrary vertical scale in Figure 7. Points at wavelengths greater than 1 mm are increasingly uncertain since the signal from both systems is very small because of low spectrometer output. The solid curve shows the predicted attenuation due to the blocking material, which indicates that the bolometer response is uniform over the range 300 to 1000 μ , as expected from the theoretical curves in Figure 2. At shorter wavelengths the bolometer response cannot be determined. The overall system response clearly decreases at longer wavelengths, but because of the low accuracy of the points it is impossible to say what this is due to. This detector system was used to test some of the filters constructed in part (2) of the program, because of its greater sensitivity compared to the Golay cell.

MILLIMETER SYSTEM RESPONSE

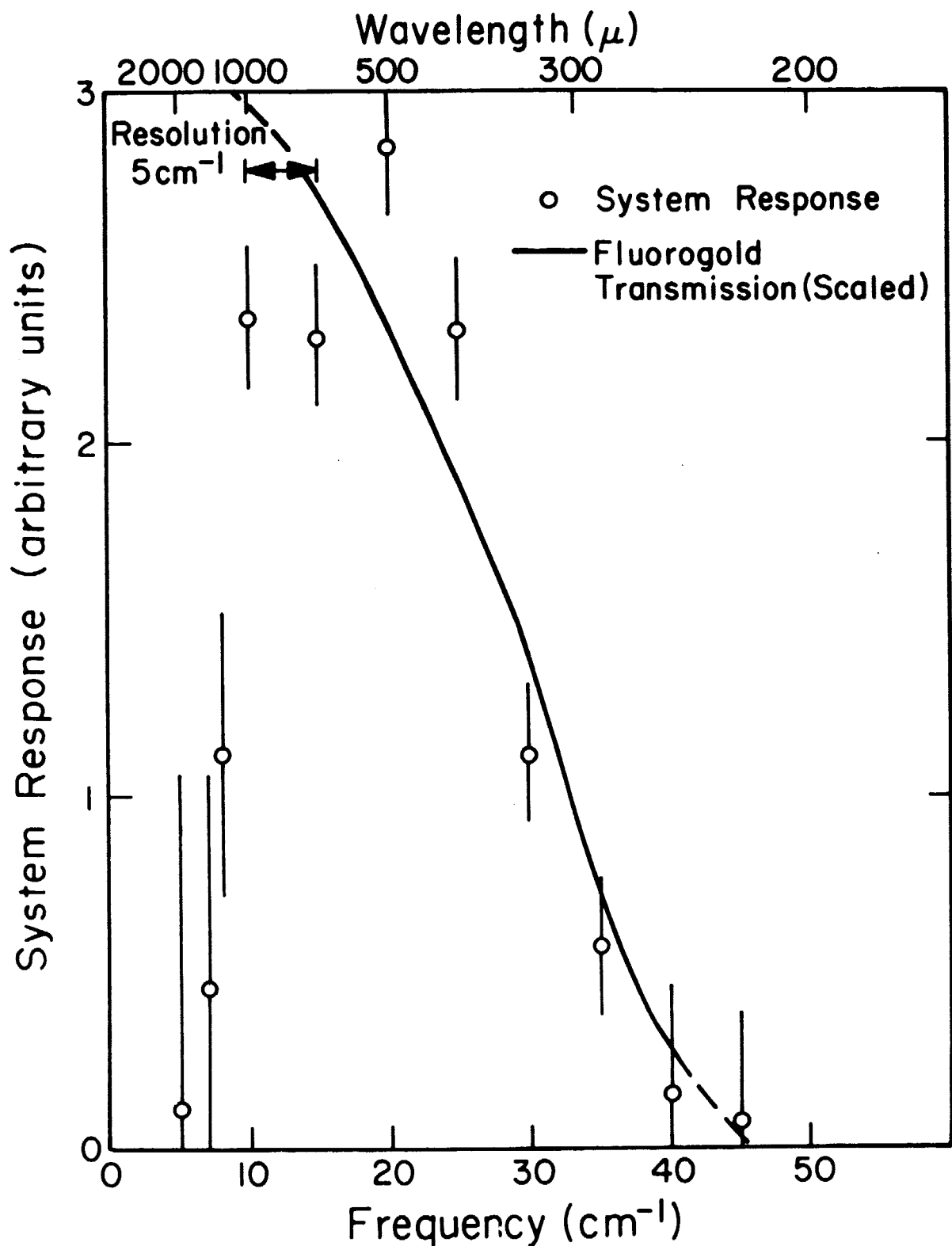


Figure 7: Overall Wavelength Response of System Shown in Figure 6.

B. Filter Design and Construction

Our filter construction program involved designing test filters and then attempting to construct them. The design techniques are straightforward, and can be found described in many of the references given previously. Those most useful are Moller and Rothschild (1971) and the paper by Holah and Smith (1972).

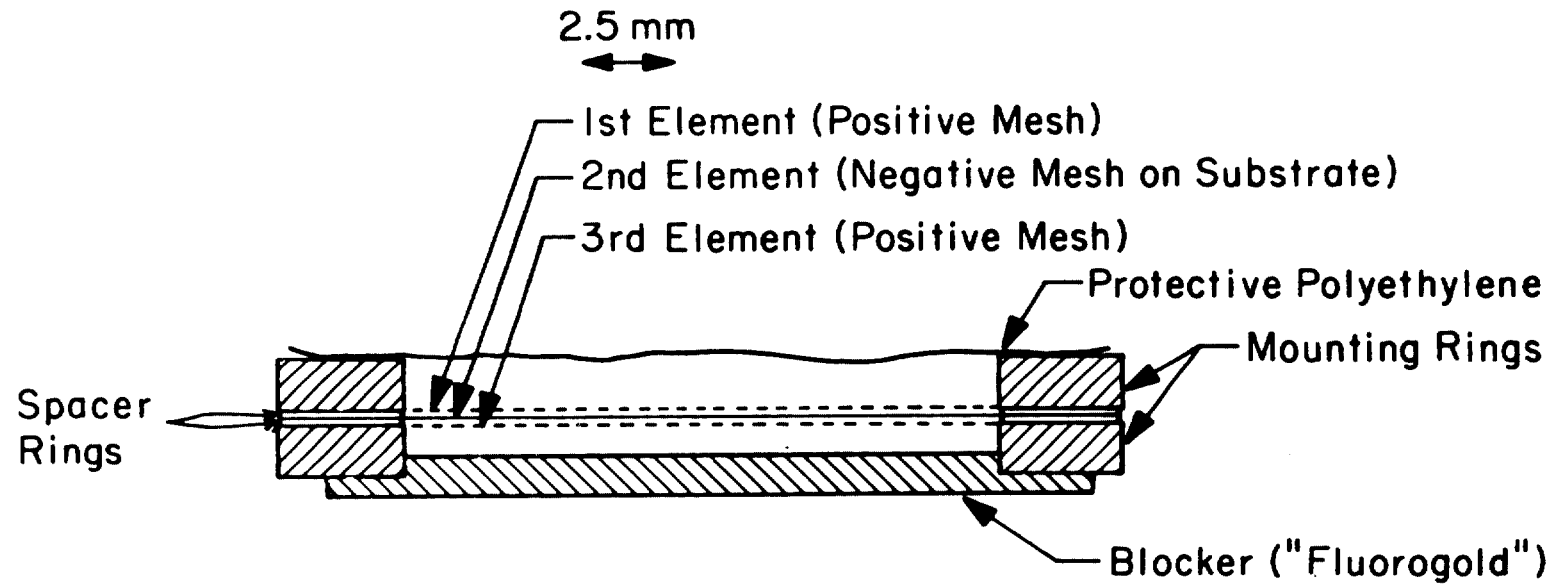
Our construction technique was straightforward. The filter consists of two or more elements separated by brass spacers and stretched over an aluminum ring. A second aluminum ring is added for rigidity and a blocking filter can be mounted on the outside of one of the rings. A typical filter is shown, enlarged in cross-section in Figure 8.

The meshes we used were of two types. The inductive meshes we used were obtained commercially.¹² These are electro-formed nickel meshes several microns thick. Though fragile, they can tolerate a small amount of stretching in order to remove wrinkles. Unfortunately, capacitive meshes are not so readily available, and we were obliged to make our own. This we did by evaporating copper onto thin (5-10 μ) mylar or polyethylene substrates, using an inductive mesh as a mask so that the actual pattern on the substrate was the complement of the inductive mesh. With the small evaporator available to us, we could make only one element at a time, so in designing filters we tended to minimize use of capacitive meshes.

The spacers we used were ordinary brass shim stock, which we found to be flat to $\pm 3 \mu$ or better over areas of a

¹²Buckbee-Mears, Minneapolis, Minnesota

TYPICAL FILTER (3 ELEMENTS) (Cross-Section)



Positive Mesh Pattern

Negative Mesh Pattern

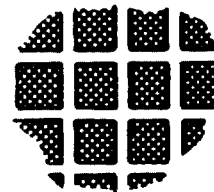
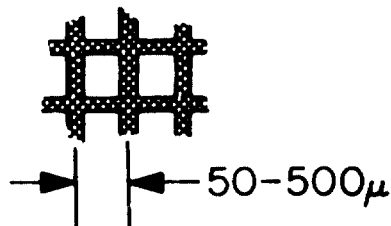


Figure 8: Schematic of Typical Filter

few square inches. The flatness tolerances set a limit on the narrowness of the band which can be produced. The flatness requirement for spacers is about 0.1 times the bandwidth, so our filters were limited to bandwidths greater than about 50 μ . Absolute thickness was less accurate, deviating from nominal by as much as 10 μ , though generally less. In the relevant thickness range (100-500 μ) shim stock is readily available in 25 μ multiples. Since spacers are typically about half a wavelength in thickness, this meant that a peak wavelength for the filter could only be selected to within about 30 μ .

Holah and Smith worked successfully at 100 μ with spacers they etched to the necessary thicknesses and tolerances, so it is possible to use this general technique at shorter wavelengths than we did.

Our assembly technique was simple. We first loosely stretched the elements of the filter across individual rings and glued them in place. We then placed a mounting ring on a jig. The first element was laid over this ring and stretched tightly, then glued in place. The first spacer was then laid on top of the mesh element and glued down. Successive mesh elements and spacers are then stretched and glued down, and a second mounting ring is placed on top of the last mesh element. Registration of the meshes is unimportant. A weight is applied to the filter to squeeze excess glue from between the elements and spacers.

It is of course essential that the glue be fairly dilute and dry slowly enough that the filter can be completely assembled while the glue on the first element is still wet. We used GE varnish¹³ diluted 2:1 or even 3:1 in acetone, but any adhesive with similar properties would work out as well.

¹³General Electric No. 7031 Varnish

C. Results

Using this technique, we have constructed (to date) about thirty filters. Roughly half of these were rejected, mostly because the meshes were not flat enough in the final filter. Figures 9, 10 and 11 show the transmission curve of four of our better filters. All filters were tested on the FS 720 spectrometer described previously, using either the Golay cell or a composite bolometer as the detector. Table I lists the mesh and spacer parameters.

Figure 9 shows an example of the simplest type of filter to construct: a long wavelength cut-off filter. This particular filter is of interest because it is one of the first filters constructed, and because it has been used for astronomical observations for a period of about two years. The filter is designed to eliminate wavelengths longer than $500\ \mu$, and is intended to be used as a blocking filter for $350\ \mu$ observations, where the atmosphere provides a short wavelength cut-off. For the ST, short wavelength blocking would have to be provided by a blocking filter. Theoretical transmission for this (and all other mesh filters) should be over 90 per cent. The lower value found in actual filters is due to lack of flatness in the meshes. Filters made later according to the same design have had peak transmissions as high as 90 per cent.

Figures 10 and 11 show examples of narrower bandpass filters, where the initial short wavelength cut-off is provided by the filter itself. All three filters incorporate a blocking filter made of Fluorogold⁹ in order to further reduce the transmission in the second and higher orders. Because these three filters contain three elements, including one of our capacitive meshes, the peak transmission is reduced

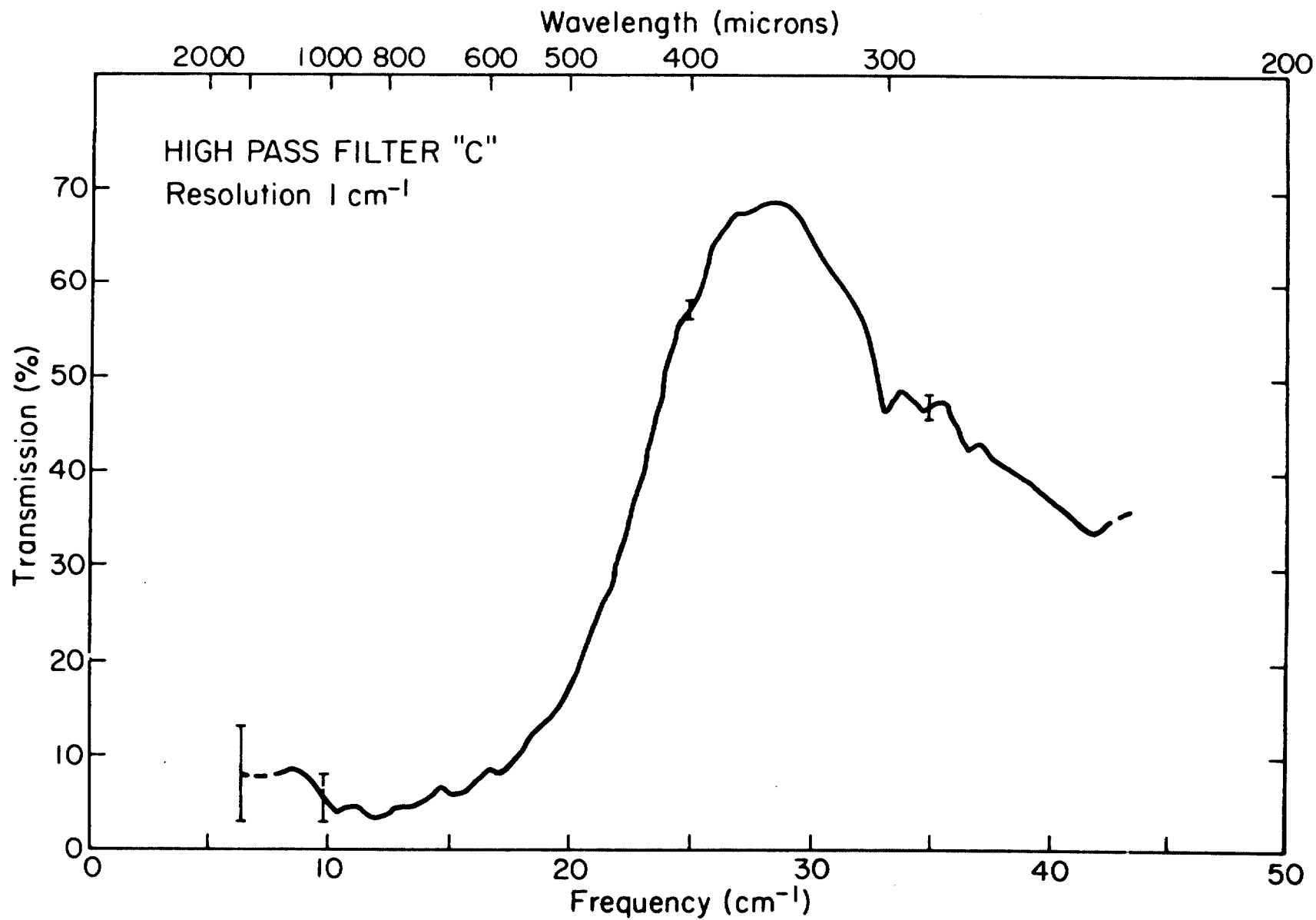


Figure 9. Transmission Curve
for High Pass Filter

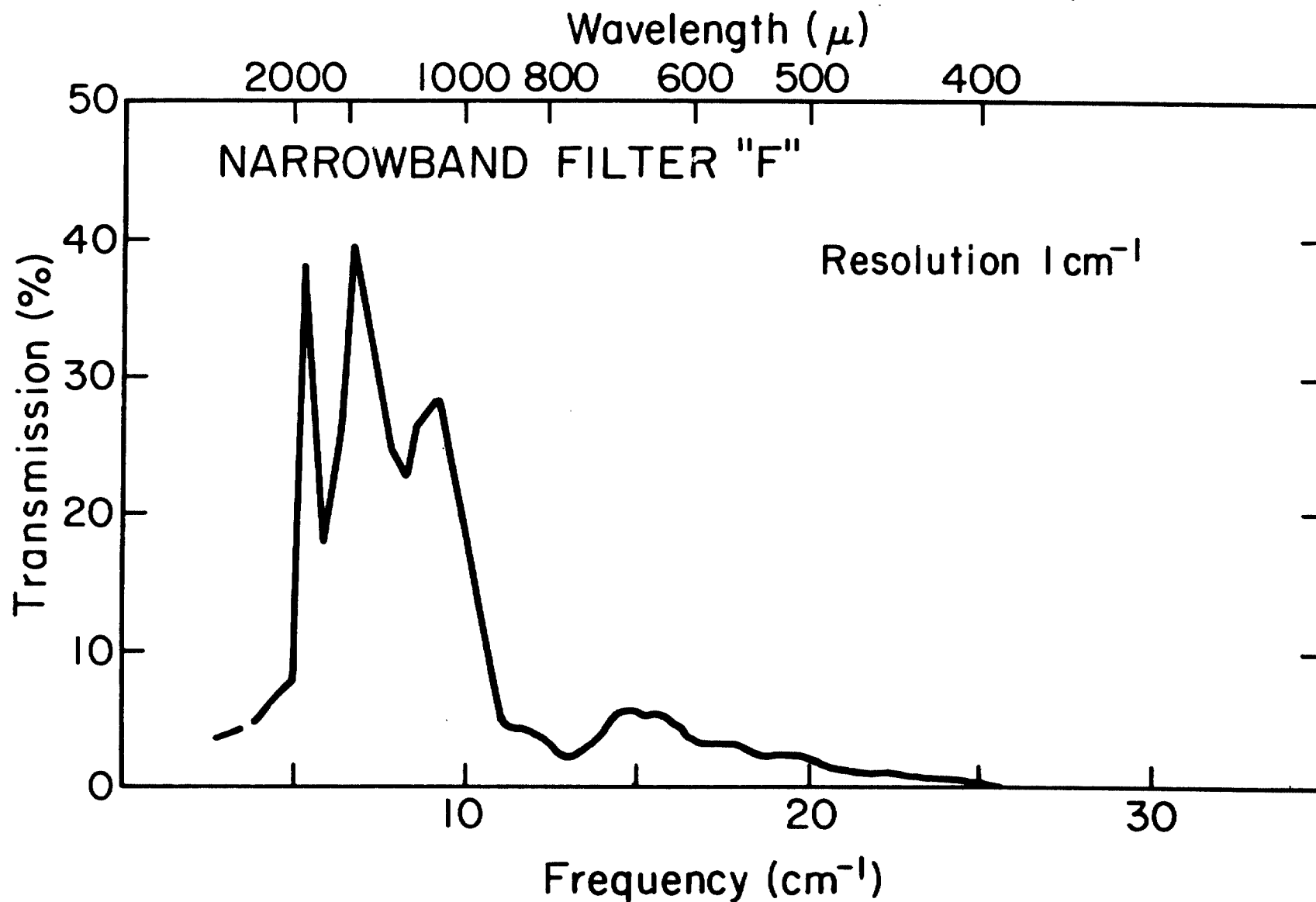


Figure 10. Transmission Curve
for Narrow Band Filter

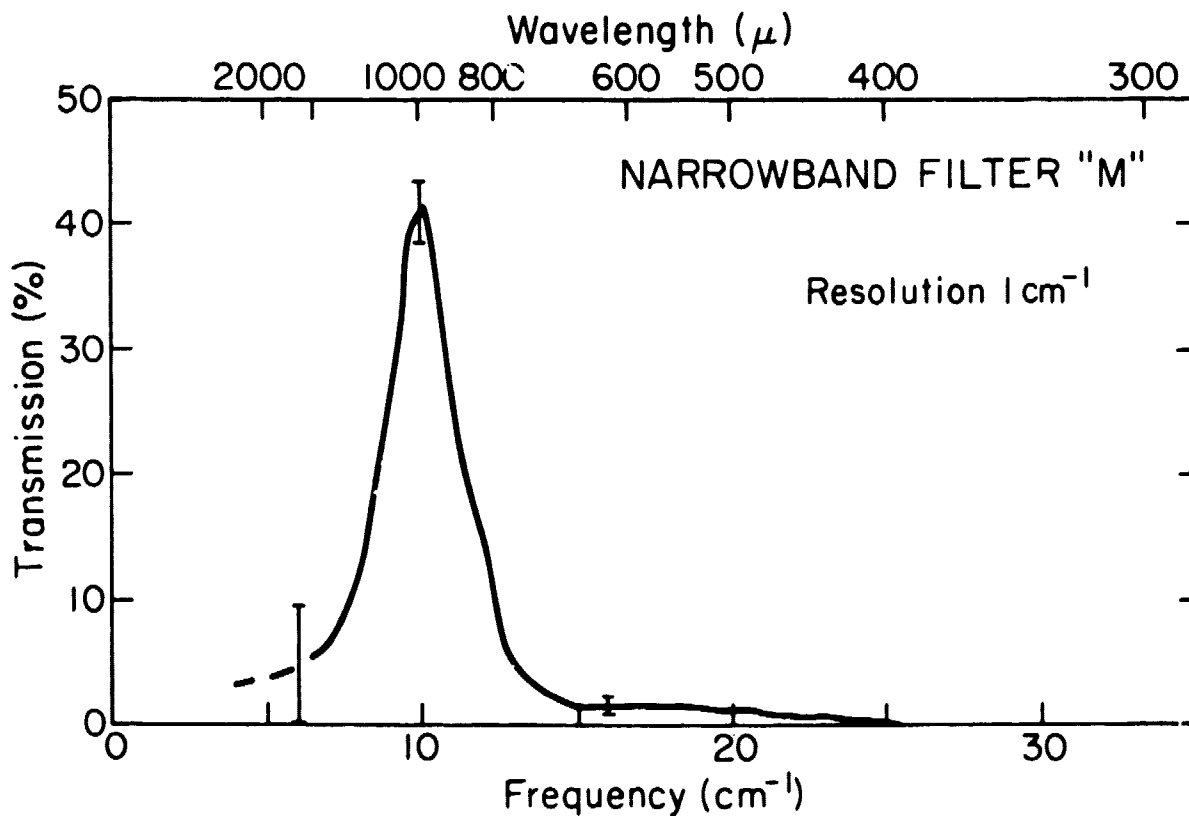
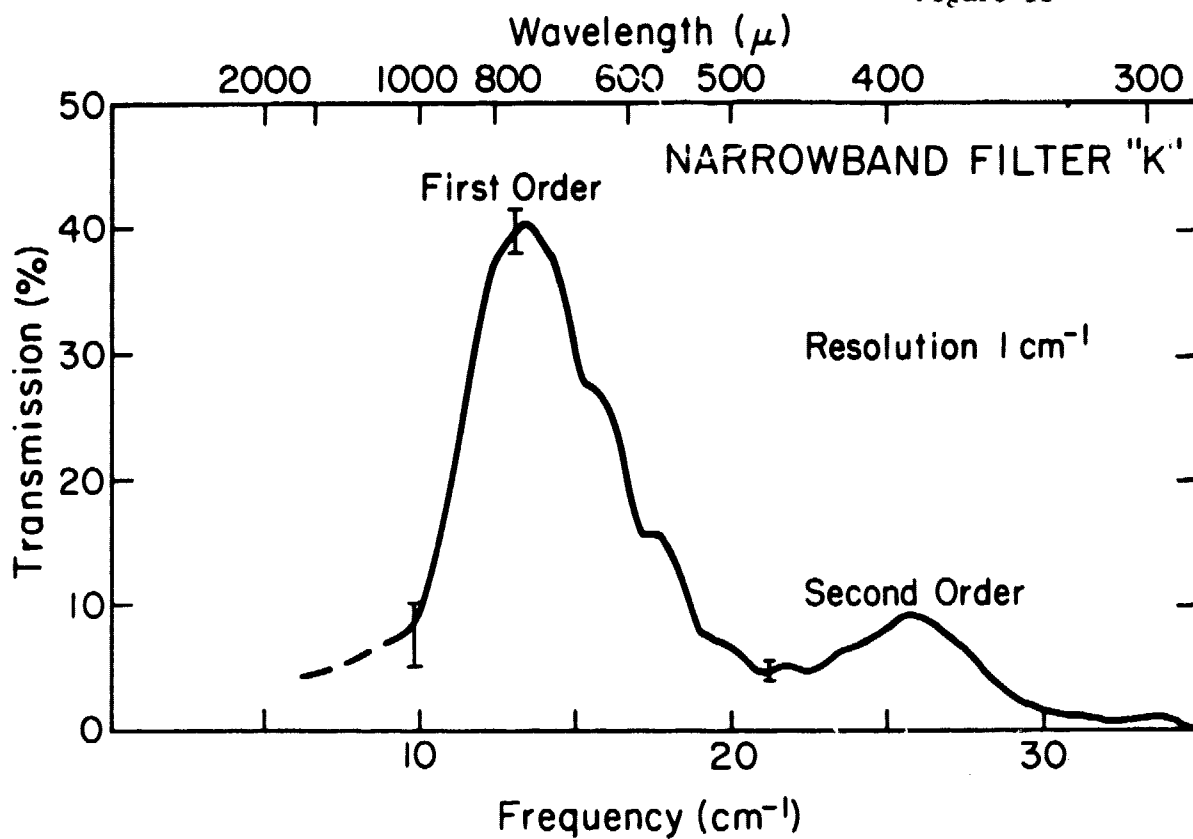


Figure 11: Transmission Curves
for Narrow Band Filters

to about 40 per cent. Because of low detector response, the transmission curves are uncertain beyond about $1500\ \mu$. These three filters have also survived about a year-and-a-half of trips to, and use at the telescope, though only "M", the 1 mm filter has been used for measurements (Westbrook et al. 1976).

III. Commercially Available Filters

At the time we began work under this contract, several companies appeared to be marketing filters of the general type described here. We ordered a filter, using contract funds, with a 10 per cent bandwidth at $50\ \mu$ from the company (Edinburgh Instruments, Ltd.) which had advertised the specifications most closely approaching the filters desired for the ST. The filter, when delivered, proved unsatisfactory because it did not have the proper central wavelength and because there was no blocking provided for out-of-band rejection. This filter was returned to the manufacturer and has not been sent back to us. Based on this and other experiences, we feel that reliable commercially manufactured filters are not currently available for this wavelength region.

IV. Summary

It is clear from our work that design of filters is straightforward, and actual assembly fairly simple. However, any manufacture of filters on a large scale, as needed for the ST, requires solution of a number of problems.

- (1) Spacers are needed which are flat to perhaps $1\ \mu$ (for the thinner sizes) and which can have thicknesses specified to similar accuracies.

(2) A superior setup for production of capacitive meshes is needed, or else designs for filters should eliminate their use almost entirely. Because capacitive mesh elements help block out the second and third orders of filters, this implies some investigation directed toward finding superior blocking materials for long wavelengths.

(3) In any case, some work on long wavelength blocking materials would probably be worthwhile.

Additionally, an interesting possibility was suggested to us by our work. If the meshes could be embedded and accurately spaced in a plastic matrix, the durability of these filters would be greatly increased. The filters used by Muehlner and Weiss (1973) were constructed in this way, although they were long wavelength-pass rather than bandpass filters and were thus subject to less critical tolerances. Also, if Yoshinaga filters are used as blocking filters, these could then be bonded onto the narrow-band component or even included in the embedding matrix itself.

TABLE 2 - Filter Parameters

Filter Name	First Element	Spacer (μ)	Second Element	Spacer (μ)	Third Element
C	125 lpi* Inductive	135	125 lpi Inductive		
F	50 lpi Inductive	500	50 lpi Inductive	670	70 lpi Capacitive
K	80 lpi Inductive	355	125 lpi Capacitive	355	80 lpi Inductive
M	50 lpi Inductive	670	70 lpi Capacitive	670	50 lpi Inductive

All four filters were 1 inch diameter. The inside diameter of the spacers is approximately 15 mm (0.6 in).

* lines per inch

BIBLIOGRAPHY

- Armstrong, K. R. and Low, F. J. Applied Optics. 12, 2007, 1973.
- Armstrong, K. R. and Low, F. J. Applied Optics. 13, 425, 1974.
- Clarke, J., Hoffer, G. I. and Richards, P. L. Revue de Physique Appliquee, 9, 69, 1974.
- Coron, N., Dambier, G. and LeBlanc, J. Infrared Detection Techniques for Space Research, edited by Manno and Ring, (D. Riedel Publishing Company), p. 121, 1972.
- Hauser, M. G. and Notarys, H. A. Bull. Am. Astron. Soc. 1, 409, 1975.
- Holah, G. and Smith, S. Journal of Physics D, 5, 496, 1972.
- Low, F. J. J. Opt. Soc. Am. 51, 1300, 1961.
- Low, F. J. Cryogenics and Infrared Detection (Boston Technical Publishers) p. 21, 1970.
- Moller, K. and Rothschild, W. Far-Infrared Spectroscopy, (Wiley Interscience), 1971.
- Muehlner, D. and Weiss, R. Phys. Rev. D., 7, 326, 1973.
- Werner, M. W., Elias, J. H., Gezari, D. Y., Hauser, M. G. and Westbrook, W. E., Ap. J. (Letters), 199, L185, 1975.
- Westbrook, W. E., Werner, M. W., Elias, J. H., Gezari, D. Y., Hauser, M. G., Lo, K. Y. and Neugebauer, G. Ap. J. 209 1976.
- Wijnbergen, J. Astronomy and Astrophysics, 29, 159, 1973.